# Time-Resolved Small-Angle X-ray Scattering Studies on the Kinetics of the Order–Disorder Transition of Block Polymers. 1. Experimental Technique

**Takeji Hashimoto,* Keisuke Kowsaka,† Mitsuhiro Shibayama,‡ and Shoji Suehiro**

*Department of Polymer Chemistry, Faculty of Engineering, Kyoto University, Kyoto 606, Japan.* *Received June 25, 1985*

ABSTRACT: Time-resolved small-angle X-ray scattering (SAXS) was used to analyze transient structural responses at a time interval on the order of seconds. As an application of the technique, we present here kinetic studies of the order–disorder transition (i.e., the microphase dissolution) of block polymers induced thermally by a temperature jump ($T$ jump). Quantitative and critical tests of the $T$-jump and time-resolved SAXS methods are presented.

## I. Introduction

Block polymers comprising two amorphous polymers (A–B, A–B–A, etc.) form a microdomain structure in the strong-segregation limit, in which the Flory–Huggins thermodynamic interaction parameter $\chi$ between the constituent chains A and B satisfies

$$\chi N > (\chi N)_c \tag{1}$$

In eq 1, $N$ is the total degree of polymerization of the entire block polymer and $(\chi N)_c$ is the critical value of $\chi N$ above which the microdomain structure is thermodynamically stable (ordered state). When the temperature is raised (if the system has an upper critical solution temperature (UCST)) or lowered (if the system has a lower critical solution temperature (LCST)), $\chi$ decreases and the condition $\chi N < (\chi N)_c$ is satisfied, resulting in dissolution of the domains into a disordered molecular mixture of A and B.[1-7] In this condition the molecular mixture rather than the microphase-separated domains is thermodynamically stable (disordered state). In this paper we use time-resolved small-angle X-ray scattering (SAXS) to investigate the kinetics of the order–disorder transition of block polymers thermally induced by a temperature jump ($T$ jump).

In previous papers,[8] we presented the principle of time-resolved SAXS to study the order–disorder transition of block polymers and gave preliminary experimental results. In this paper we focus our attention on quantitative and critical tests of the time-resolved SAXS and $T$-jump methods. Especially, the effects of finite time to achieve the $T$ jump on the analyses and related necessary corrections will be discussed.

## II. Experimental Technique

**1. Specimens.** The test specimen employed was an SB diblock polymer of polystyrene (PS) and polybutadiene (PB) having a number-average molecular weight $M_n = 5.2 \times 10^4$ and a weight fraction of PS $W_{PS} = 0.30$. The solvent $n$-tetradecane (designated as C14) was added to SB to lower the order–disorder transition temperature ($T_r$). The solvent is poor for PS but good for PB.

**2. Apparatus.** Time-resolved SAXS experiments were conducted by using a specially constructed apparatus designed for high-speed measurements of SAXS profiles. The apparatus has a 12-kW rotating-anode X-ray generator and a linear position-sensitive proportional counter (PSPC) (Rigaku Denki) as described elsewhere.[9] Figure 1 is a schematic diagram of the optical setup of the SAXS apparatus constructed in our laboratory. The X-ray beam, radiating from a point focus 1 mm in diameter, was monochromatized by a flat graphite monochromator. The beam was collimated by a pair of slits 0.2 mm in width and 3 mm in height. The scattered X-ray beam was detected by a PSPC placed 1130 mm from the sample. The full-widths at half-maxima for the slit-height and slit-width weighting functions are, respectively, 9.17 and 1.31 mrad or 0.37 and 0.054 $nm^{-1}$ in units of the scattering vector as defined by

$$q = (4\pi/\lambda) \sin \theta \tag{2}$$

where $\lambda$ is the wavelength of the radiation (Cu K$\alpha$, 0.154 nm) and $2\theta$ is the scattering angle. The slit-height weighting function was relatively narrow, so further desmearing correction was not performed in this study.

Time-resolved SAXS profiles were detected by a linear PSPC, position-analyzing electronics, and two-parameter multichannel analyzer (MCA) with a 16-kiloword (16 bits/word) memory area available for scattering data.[9]

**3. Time-Resolved SAXS Method.** Figure 2 shows the temperature-jump method employed in this study. The specimens were installed in a small aluminum holder with a relatively small heat capacity (Figure 2a). Typical sample space dimensions were 3-mm width, 10-mm length, and 2-mm thickness, and both sides of the windows were sealed by thin polyester films 2 $\mu$m thick (Figure 2b). The small aluminum holder itself was held by an insulating material made of poly(tetrafluoroethylene) (Teflon) (Figure 2b). The specimens were initially maintained in a heated block where temperature was controlled at initial temperature $T_i$. The holder was then rapidly transferred manually into another heated block which was set in the optical system of SAXS experiments and regulated at the measuring temperature $T_m$ (Figure 2c).

Insertion of the specimen holder into the heated block at $T_m$ triggered the data acquisition of SAXS profiles by the two-parameter MCA, according to the preprogrammed time schedule shown in Figure 3. In temperature-jump ($T$-jump) experiments, the temperature of the specimens was rapidly elevated from $T_i$ to $T_m$. In kinetic studies of the order–disorder transition of the block polymers, $T_i$ and $T_m$ were set respectively below and above $T_r$, the order–disorder transition temperature. In the temperature-drop ($T$-drop) experiments, $T_i$ and $T_m$ were set above and below $T_r$, respectively.

Repetitive $T$-jump and $T$-drop methods were employed to improve the statistical accuracy of the X-ray photon counting. For example, in the $T$-jump experiments, the temperature was rapidly elevated from $T_i$ to $T_m$, and the first dynamic SAXS experiments (i.e., the time-resolved SAXS experiments) were performed during time $t_D$. The temperature was then slowly lowered to the initial temperature $T_i$ and kept at that temperature for a sufficient period to recover the original microdomain structure.[10] Then the temperature was again rapidly elevated from $T_i$ to $T_m$, and the second dynamic experiments were carried out. The dynamic experiments were repeated $R$ times. At the end of the $T$-jump experiments, static SAXS measurements were carried out at $T_m$.

In each dynamic experiment, the change in the SAXS profiles with time after a $T$ jump or $T$ drop was measured with $N$ time

† Present address: Textile Research Laboratory, Asahi Chemical Industry Co., Ltd., Takatsuki, Osaka 569, Japan.

‡ Present address: Department of Polymer Science and Engineering, Kyoto Institute of Technology, Matsugasaki, Kyoto 606, Japan.

0024-9297/86/2219-0750$01.50/0 

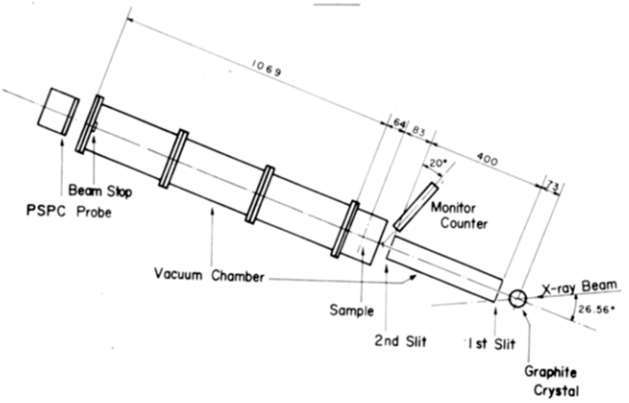


**Figure 1.** Schematic diagram of SAXS optics with a linear position-sensitive proportional counter (PSPC).

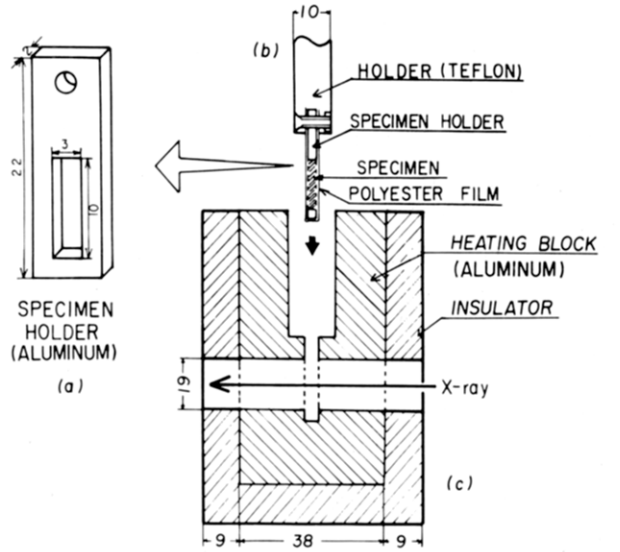


**Figure 2.** Specimen holder (a, b) and heated block (c) used in the temperature-jump experiments.

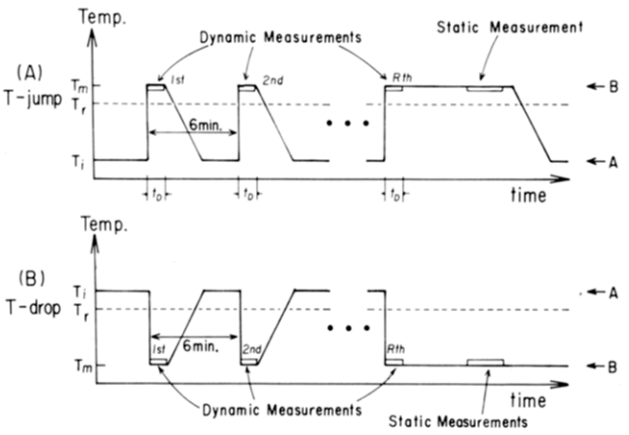


**Figure 3.** Temperature programs for repetitive temperature-jump (a) and temperature-drop (b) experiments.

slices, each time slice having a time period of $t_p = t_D/N$. In this experiment the preset time $t_p$ was 2 s, and $R$ was set at 10. The data corresponding to the time-resolved SAXS profiles were stored in the two-parameter MCA, where 256 channels were used to store the SAXS profile at a given time slice, and the time variation of the profiles was recorded over 64 time slices.

The temperature change of the sample with time after the $T$ jump was measured by embedding a thermocouple in the sample. The temperature change was sigmoidal and approximated by

$$T(t) = T_m - (T_m - T_i) \exp(-t/\tau) \quad (3)$$

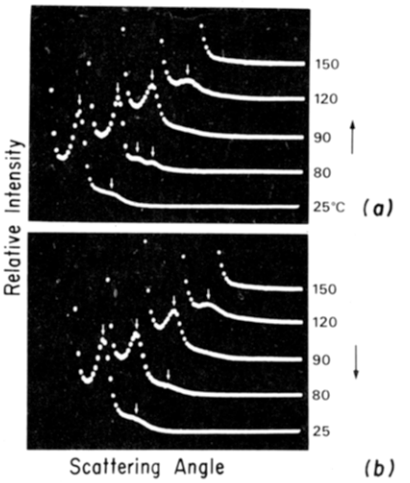


**Figure 4.** Oscilloscope displays of change of the static SAXS profiles with temperature during (a) heating and (b) cooling cycles. Origin of each curve is shifted diagonally to avoid overlap. The number attached to each curve represents temperature in degrees centigrade.

where the retardation time $\tau$ was detected to be 6 s. In order to reduce $\tau$, a tight contact between the small specimen holder and the heating block was found to be extremely important. This retardation time $\tau$ may reasonably correspond to the time required for heat conduction $t_H \simeq X^2/2D_T$, where $X$ corresponds to the distance over which the heat is transferred and $D_T$ is the thermal diffusivity. In these experiments $X \simeq 10^{-1}$ cm and $D_T \simeq 5 \times 10^{-4}$ cm$^2$/s; hence $t_H \simeq 10$ s, ensuring $t_H \simeq \tau$.

## III. Results

The change of static SAXS profiles with temperature was extensively studied in our earlier work.[11] Here we qualitatively present in Figure 4 a typical example for the system 35 wt % SB in C14. Figure 4 shows oscilloscope displays of the changes of the SAXS profiles with temperature during heating (a) and cooling cycles (b), where origins of the profiles are shifted diagonally to avoid overlap.

The scattering maxima marked by arrows are attributed to interparticle interference maxima of spherical polystyrene domains in a simple cubic-like superlattice in the matrix of polybutadiene solutions.[11] When temperature is increased, the maxima first become broad and then disappear or become indistinct. When temperature is decreased from a temperature above 150 °C, the maxima first appear or become distinct and then become sharp. The thermally reversible changes of the SAXS profiles with temperature were found to manifest thermally reversible structural changes of the block polymer systems: for increasing temperature, a disordering of the superlattice is first observed followed by dissolution of the spherical microdomains; for decreasing temperature, formation of the microdomains and then ordering of the superlattice are observed.[11] The lattice disordering (lattice ordering) is related to broadening (narrowing) of the maxima, and the dissolution (formation) of the microdomains is related to disappearance (appearance) of the maxima. Detailed analyses described in a companion paper[12] indicated $T_r$ (the order–disorder transition temperature) for the system is 120 ± 5 °C.

It should be noted that a weak and broad scattering maximum was found to exist even at temperature above $T_r$ by careful observations with a prolonged measuring time and an amplified intensity scale. This maximum is attributed to thermal fluctuations of the block polymer in the disordered state of the type theoretically investigated by de Gennes,[13] LeGrand,[14] Leibler,[1,15] and Benoit[15,16] and

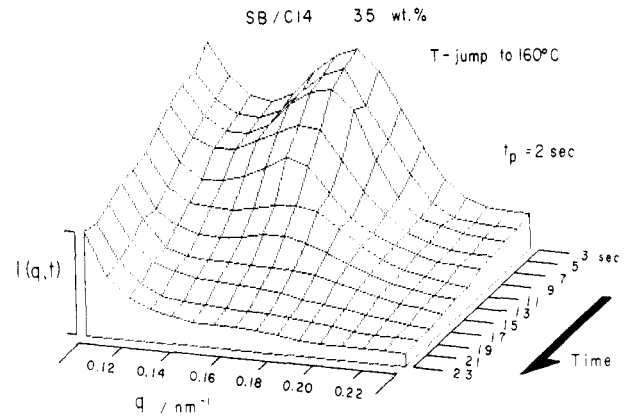


**Figure 5.** Isometric display showing typical variations of SAXS profiles with time after a temperature jump. $T_i$ = 25 °C, $T_m$ = 160 °C, $t_p$ = 2 s, and $R$ = 10 for a 35 wt % SB solution in C14.

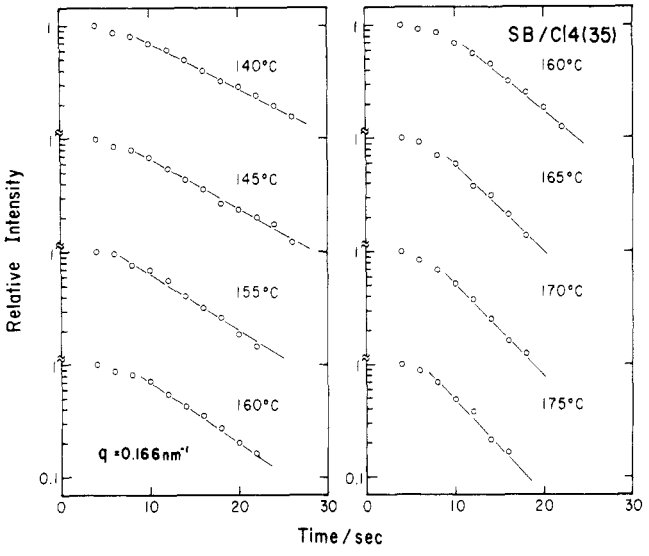


**Figure 6.** Decay of scattered intensity at $q$ = 0.166 nm$^{-1}$ with time after a temperature-jump at various $T_m$'s for a 35 wt % SB solution in C14. log $[I(q,t;T_m)/I(q,t=0;T_m)]$ vs. $t$.

experimentally by Roe et al.,[2] Hashimoto et al.,[3-6] and Bates.[7]

Figure 5 presents an isometric display for the time-dependent variation of the SAXS profiles after the $T$ jump from room temperature to 160 °C for 35 wt % SB solution in C14. The real-time analyses were carried out by the time-resolved SAXS method with a repetitive $T$-jump program, $t_p$ and $R$ being set equal to 2 s and 10, respectively.

Figure 6 shows the change in scattered intensity at $q$ = 0.166 nm$^{-1}$ (close to the scattering vector giving rise to the maximum intensity) with time at various measuring temperatures $T_m$ (above $T_r$) for the same solution as in Figure 5. The semilogarithmic plot at each temperature indicates that the intensity decay is faster at higher $T_m$ and that the decay is initially nonexponential but later exponential. The rate of intensity decay is faster at higher temperature. We discuss the significance of these data in the next section.

## IV. Theoretical Analyses

We have presented a theoretical basis upon which the time-resolved SAXS profiles during the order–disorder transition of block polymers can be treated.[8] The $T$ jump from $T_i$ to $T_m$ above $T_r$ invokes dissolution of the phase-separated microdomains into a homogeneous molecular mixture as a consequence of the energetics causing the segregation of A and B macromolecules being outweighed by the entropy causing a random placement of chemical junctions of A and B in A–B block polymers and a random mixing of A and B. This dissolution is attained by Brownian motion of centers of block polymer molecules at $T_m$. The translational diffusion of the molecular centers, in turn, causes mutual diffusion of the A and B segments, resulting in a change of the spatial segmental density profiles with time $\rho_K(\mathbf{r},t)$ ($k$ = A or B).

For the case where the repulsive thermodynamic interaction between A and B does not significantly affect the diffusional flux of A and B segments at $T_m$, we found

$$\rho_K(\mathbf{r},t) = \rho_K(\mathbf{r},t=0)*h_j(\mathbf{r},t) \qquad (k = \text{A, B}) \tag{4}$$

$$h_j(r,t) = \left[\frac{j}{2\pi\sigma_j^2}\right]^{j/2} \exp[-jr^2/2\sigma_j^2] \tag{5}$$

and

$$\sigma_j^2 = 2jD_c t \qquad (j = 1, 2, 3) \tag{6}$$

where the asterisk denotes convolution product, $D_c$ is the diffusivity for the center-of-mass of the block polymers, $j$ is an integer related to dimensionality, and $\rho_K(\mathbf{r},t=0)$ is the spatial segment-density profile immediately after the $T$ jump. Physically, $h_j(\mathbf{r},t)$ describes the change of the spatial distribution of the molecular center with time. For the case where the interaction plays an important role for the mutual diffusion, $D_c$ should be substituted by an effective diffusivity $D_{eff}$ which is a function of $D_c$ and the interaction parameter $\chi$. The change of the density profile causes the change of the elastic scattered intensity profile $I(q,t)$

$$I(q,t) = I(q,t=0) \exp[-2q^2D_{eff}t] \tag{7}$$

where $I(q,t=0)$ is the scattered intensity profile immediately after the $T$ jump.

**1. Ideal One-Step $T$-Jump Process.** Equations 4–7 do not include the effect of random thermal noise on $\rho_K$ and $I(q,t;T_m)$. Thus at $t \to \infty$, $\rho_K$ becomes uniform and $I(q,t;T_m)$ becomes zero. In reality the scattered intensity never drops to zero due to thermally induced concentration fluctuations occurring in the disordered state. If the scattered intensity due to the fluctuations is defined as $I_s(q;T_m)$, then

$$\lim_{t\to\infty} I(q,t;T_m) = I_s(q;T_m) \tag{8}$$

Thus, in order to analyze semiquantitatively the experimental data, eq 7 was modified as follows:

$$I(q,t;T_m) = [I(q,t=0;T_m) - I_s(q;T_m)] \exp(-2q^2D_{eff}t) + I_s(q;T_m) \tag{9}$$

**2. Nonideal $T$-Jump Process: Approximation of Multistep $T$-Jump Process.** The $T$ jump does not involve stepwise temperature change from $T_i$ to $T_m$ but rather the sigmoidal variation as characterized by eq 3 with $\tau$ = 6 s. This effect of the retarded temperature change on the decay of the scattered intensity $I(q,t;T_m)$ is analyzed here on the basis of a multistep temperature jump as schematically shown in Figure 7. In this approximation, each elemental step, e.g., the $T$ jump from $T_j$ to $T_{j+1}$ occurs ideally but the entire change from $T_i$ to $T_m$ requires time $N\Delta t$.

For example, the elemental $T$-jump process from $T_{j-1}$ to $T_j$ at time $t_j$ will cause the scattered intensity $I(q,t_j)$ at $t_j$ to result in $I(q,t_{j+1})$ at $t_{j+1}$ after a time interval of $\Delta t = t_{j+1} - t_j$

$$I(q,t_{j+1}) = [I(q,t_j) - I_s(q;T_j)] \exp[-2q^2D_{eff}(T_j)\Delta t] + I_s(q;T_j) \tag{10}$$

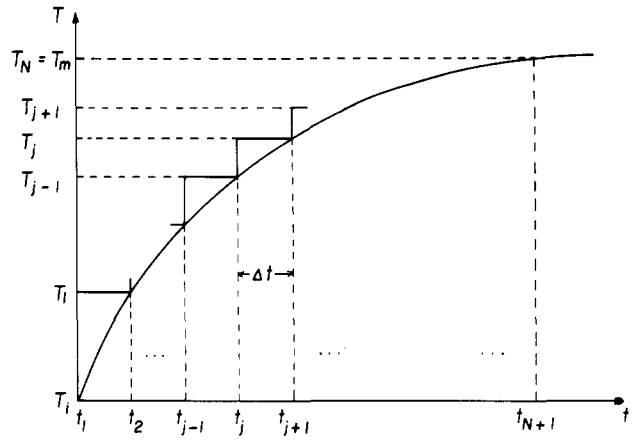


**Figure 7.** Approximation of multistep temperature-jump process.

where $I_s(q;T_j)$ is the static scattering intensity profile at $T_j$, and the running index $j$ goes from 1 to $N$ with $t_1 \equiv 0$ and $T_N \equiv T_m$. From eq 10 it follows that

$$I(q,t_{N+1}) = \sum_{j=1}^{N} [I_s(q;T_{j-1}) - I_s(q;T_j)] \exp[-2q^2 \sum_{k=j}^{N} D_{eff}(T_k)\Delta t] + I_s(T_N) \quad (11)$$

Thus if the temperature dependences of $I_s(q;T)$ and $D_{eff}(T)$ are known, one can estimate $I(q,t;T_m)$. In this work the temperature dependence of $D_{eff}$ is assumed to be given by[17]

$$D_{eff}(T) = D_0 \exp(-\Delta H_a/RT) \quad (12)$$

and $I_s(q;T)$ was experimentally measured. Thus for a given temperature history of eq 3, $I(q,t;T_m)$ can be estimated if $D_0$ and $\Delta H_a$ are known. It is obvious from eq 10 and 11 that if the diffusivity is infinitely large

$$I(q,t_{j+1}) = I_s(q;T_j) \quad (13a)$$

and

$$I(q,t_{N+1}) = I_s(T_N) \quad (13b)$$

Hence the scattered intensity at a given time is equal to the static intensity at the corresponding temperature.

Figure 8 presents results of numerical calculations of $I(q,t;T_m)/I(q,t=0;T_m)$ based on eq 10 or 11. In the calculations, the following conditions were set: $T_i$ = 25 °C, $T_m$ = 150 °C, $D_{eff}(T_m$=150 °C) = 2.0 nm²/s, $\Delta H_a$ = 9.0 kcal/mol, and $q$ = 0.166 nm$^{-1}$. The corresponding relaxation time for the decay of scattered intensity, $\tau_{qi}$, is given by

$$\tau_{qi} = (2q^2 D_{eff})^{-1} = 9.05 \text{ s} \quad (14)$$

The calculations were carried out for various retardation times $\tau$ for the temperature change. The ideal $T$-jump process which corresponds to $\tau = 0$ gives rise to the exponential decay of the scattered intensity over the entire time scale. Nonideality of the $T$-jump process as manifested by nonzero values of $\tau$ gives nonexponential decay of the scattered intensity in the initial stage of the transition as found in the experimental results shown in Figure 6. However, in the time scale of $t \gg \tau$, the intensity decays exponentially, irrespective of the value $\tau$, at the same rate $R(q)$

$$R(q) = 2q^2 D_{eff} = \tau_{qi}^{-1} \quad (15)$$

The larger the retardation $\tau$, the longer the time scale where the intensity decay is nonexponential. The exponential decay of the scattered intensity in the later stage was also found in the experimental results shown in Figure 6.

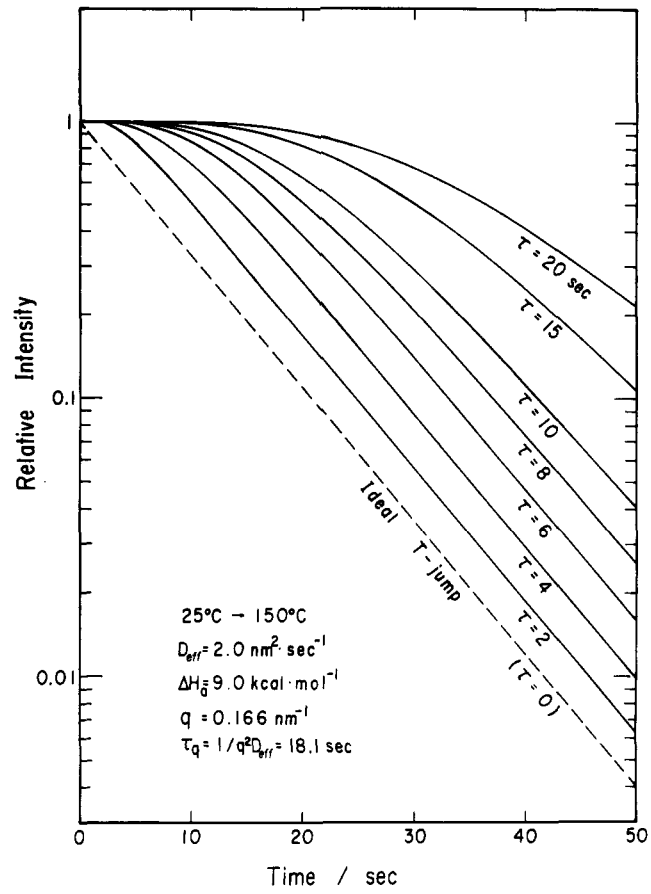


**Figure 8.** Effects of retarded temperature jump on intensity decay with time. $T_i$ = 25 °C, $T_m$ = 150 °C, $D_{eff}$ = 2.0 nm²/s, $\Delta H_a$ = 9.0 kcal/mol, and $q$ = 0.166 nm$^{-1}$. $\tau$ is the retardation time as defined by eq 3.

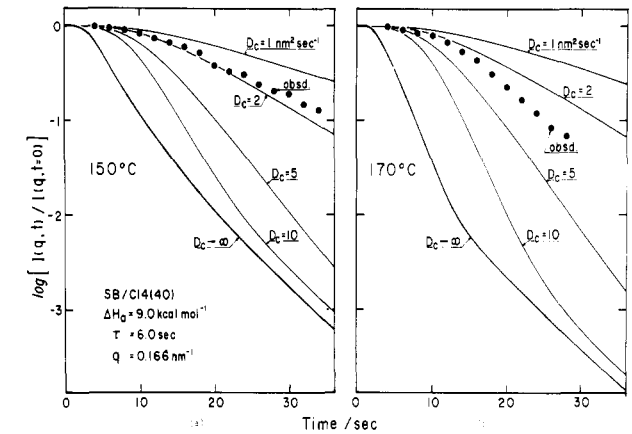


**Figure 9.** Comparison between measured and calculated intensity decay (a) at 150 °C and (b) at 170 °C for a 40 wt % SB solution in C14. The best fit gives $D_{eff}$, which corresponds to $D_c$ in the figure. $T_i$ = 25 °C, $\tau$ = 6.0 s, and $q$ = 0.166 nm$^{-1}$. The curve estimated for $D_c \to \infty$ represents the decay of the static scattered intensity with temperature after a temperature change with time as characterized by eq 3.

**3. Comparison with Experimental Results and Estimation of the Effective Diffusivity.** In this section we carry out computer simulations of the experimental decay behavior of the scattered intensity after a $T$ jump on the basis of eq 10 or 11 in order to evaluate $D_{eff}$. Figure 9 presents the observed intensity decays (filled circles) at $T_m$ = 150 °C (a) and 170 °C (b) for a 40 wt % SB solution

in C14 and the corresponding calculated results (solid lines) for various values of $D_{eff}$. The initial temperature $T_i$ was set at 25 °C and the numerical results were obtained for $\tau = 6.0$ s, $q = 0.166$ nm$^{-1}$, and $\Delta H_a = 9.0$ kcal/mol, where $\tau$ was measured and $q$ is the scattering vector at which the intensity change was measured. The activation energy $\Delta H_a$ was measured independently from the temperature dependence of $D_{eff}$'s, which, in turn, were measured from the slope of log $I(q,t;T_m)$ vs. $t$ at $t \gg \tau$.

The numerical results for $D_{eff} \to \infty$ correspond to a fictitious case of infinitely large $D_{eff}$ for which the intensity decrease with time is a mere consequence of a reduction of static intensity after a temperature increase as characterized by eq 3. The results for $D_{eff} \to \infty$ were uniquely determined by the change of static scattered intensity with temperature, $I_s(q;T)$, and the change of temperature with time, $T(t)$. The experimental evidence that the measured intensity decay with time is much slower than the decay predicated for $D_c \to \infty$ firmly confirms that the observed decay primarily reflects the molecular diffusion process.

The best fits yield the effective diffusivities of $1.8 \pm 0.1$ and $3.0 \pm 0.1$ nm$^2$/s at 150 and 170 °C, respectively. The results agree with those determined from the slopes of log $I(q,t;T_m)$ vs. $t$ at $t \gg \tau$. The method involving the $T$-jump and time-resolved SAXS analyses now seems to be well established and useful for characterization of the kinetics and molecular dynamics of the order–disorder transition of block polymers in the time scale of as short as a few seconds. The intensity decay with time during the order–disorder transition reflects the effective diffusivity $D_{eff}$. The larger the value $D_{eff}$, the faster the rate of the intensity decay. Further quantitative studies will be presented in a subsequent paper[12] on the kinetics of the order–disorder transition as a function of temperature and concentration.

## References and Notes


(1) Leibler, L. *Macromolecules* **1980**, *13*, 1602.
(2) Roe, R. J.; Fishkis, M.; Chang, J. C. *Macromolecules* **1981**, *14*, 1091.
(3) Hashimoto, T.; Shibayama, M.; Kawai, H. *Polym. Prepr., Am. Chem. Soc. Div. Polym. Chem.* **1982**, *23* (1), 21.
(4) Hashimoto, T.; Shibayama, M.; Kawai, H. *Macromolecules* **1983**, *16*, 1093.
(5) Hashimoto, T.; Tsukahara, Y.; Kawai, H. *Polym. J.* **1983**, *15*, 699.
(6) Mori, K.; Hasegawa, H.; Hashimoto, T. *Polym. J.* **1985**, *17*, 799.
(7) Bates, F. S. *Macromolecules* **1985**, *18*, 525.
(8) Hashimoto, T.; Tsukahara, Y.; Kawai, H. *J. Polym. Sci., Polym. Lett. Ed.* **1980**, *18*, 585; *Macromolecules* **1981**, *14*, 708.
(9) Hashimoto, T.; Suehiro, S.; Shibayama, M.; Saijo, K.; Kawai, H. *Polym. J.* **1981**, *13*, 501.
(10) Hashimoto, T.; Shibayama, M.; Kowsaka, K., to be submitted to *Macromolecules* (part 3 of this series).
(11) Shibayama, M.; Hashimoto, T.; Kawai, H. *Macromolecules* **1983**, *16*, 16.
(12) Hashimoto, T.; Kowsaka, K.; Shibayama, M.; Kawai, H. *Macromolecules* **1986**, *19*, 754.
(13) de Gennes, P.-G. "Scaling Concepts in Polymer Physics"; Cornell University Press: Ithaca, NY, 1979.
(14) LeGrand, A. D.; LeGrand, D. G. *Macromolecules* **1979**, *12*, 450.
(15) Leibler, L.; Benoit, H. *Polymer* **1981**, *22*, 195.
(16) Benmouna, M.; Benoit, H. *J. Polym. Sci., Polym. Phys. Ed.* **1983**, *21*, 1227.
(17) We assume here that $\Delta H_a$ does not change below and above $T_r$. It should be noted that Chung and Lin[18] reported a discontinuity in $\Delta H_a$ for a viscous flow of SBS block polymer in the bulk around $T_r$, obtaining 22.8 and 19.4 kcal/mol below and above $T_r$, respectively. A similar discontinuity might apply to $\Delta H_a$ in our system. In our case the solvent may reduce the value of $\Delta H_a$ and hence the difference of $\Delta H_a$ below and above $T_r$.
(18) Chung, C. I.; Lin, M. I. *J. Polym. Sci., Polym. Phys. Ed.* **1978**, *16*, 545.


# Time-Resolved Small-Angle X-ray Scattering Studies on the Kinetics of the Order–Disorder Transition of Block Polymers. 2. Concentration and Temperature Dependence


**Takeji Hashimoto,* Keisuke Kowsaka,† Mitsuhiro Shibayama,‡ and Hiromichi Kawai§**

*Department of Polymer Chemistry, Faculty of Engineering, Kyoto University, Kyoto 606, Japan.*

*Received June 25, 1985*


ABSTRACT: Equilibrium and kinetic aspects of the order–disorder transition of polystyrene–polybutadiene diblock polymer solutions in *n*-tetradecane were studied as a function of polymer concentration and temperature by small-angle X-ray scattering (SAXS). The order–disorder transition temperature ($T_r$) was determined by analyzing thermal concentration fluctuations of polystyrene and polybutadiene segments as a function of temperature in the disordered state. The kinetics were studied by time-resolved measurements of SAXS profiles on the time scale of a few seconds during the order–disorder transition after a temperature jump above $T_r$. The kinetic studies gave estimations of the translational diffusivities $D_{eff}$ for the center-of-mass motion of the block polymers in the solutions and the activation energies for the diffusion process. The activation energies determined by the SAXS technique were found to be in good agreement with those determined from rheological measurements.


## I. Introduction

In this paper we investigate the temperature $T_r$ and kinetics of the order–disorder transition of polystyrene–polybutadiene diblock polymers (SB) in *n*-tetradecane (C14) using small-angle X-ray scattering (SAXS). The transition temperature was determined as a function of polymer concentration by analyzing SAXS arising from thermal concentration fluctuations of polystyrene (PS) and polybutadiene (PB) segments in the disordered state[1-3] (i.e., the state where PS and PB block chains are molecularly mixed) as a function of temperature (section IV). The theoretical background for the scattering from block polymers in the disordered state may be found in the work of de Gennes,[4] LeGrand and LeGrand,[5] Leibler,[1,6] and Benoit and Benmouna.[7]

The kinetics of the order–disorder transition was studied


† Present address: Textile Research Laboratory, Asahi Chemical Industry Co., Ltd., Takatsuki, Osaka 569, Japan.
‡ Present address: Department of Polymer Science and Engineering, Kyoto Institute of Technology, Matsugasaki, Kyoto 606, Japan.
§ Present address: Hyogo University of Education, Yashiro-cho, Kato-gun, Hyogo-ken, Japan.


0024-9297/86/2219-0754$01.50/0 